An Investigation on Hot Corrosion Behaviour of Cermet Coatings in Simulated Boiler Environment

Amandeep Singh[1] · Khushdeep Goyal[1] · Rakesh Goyal[2]

Abstract

In this research work, hot corrosion behaviour of different Cr_3C_2–NiCr coatings has been investigated. The coatings were deposited on commercially available boiler tube steel with high velocity oxy fuel thermal spraying technique. The uncoated and coated specimens were exposed to elevated temperature in a silicon tube furnace at 700 °C in molten salt environment. The thermogravimetric technique was used to compare the corrosion resistance of different coatings for 50 cycles at high temperature. The microstructures of exposed specimens were evaluated with X-ray diffraction and scanning electron microscopy with elemental compositional analysis. $10Cr_3C_2$–90NiCr and $20Cr_3C_2$–80NiCr coatings provided the higher resistance to corrosion as compared to 100NiCr and $35Cr_3C_2$–65NiCr. The formation of chromium carbide layer on the coated surface and this layer protect them from corrosion.

Keywords Corrosion · Boiler · Steel · Coating · Temperature

1 Introduction

The surfaces of alloys and metals are oxidized when they are covered with a thin film of fused salt at elevated temperature, and a porous non-protective oxide scale is formed at the surface. [1–4]. This is known as hot corrosion. Due to the presence of salt contaminants such as Na_2SO_4, NaCl, V_2O_5 at high temperature, this type of oxidation is accelerated [1, 5, 6]. Hot corrosion is also form of oxidation and these salt contaminants degrade the protective oxide layer [7, 8]. In 1940, the hot corrosion was first recognized for the degradation of the boilers tubes and steam generating plants [1, 9]. After that, this problem was observed in IC engines, gas turbines, and many industrial waste incinerators. Today the researchers have developed many efficient coatings that help to protect the materials from hot corrosion. In a coal fired boiler, many failures occur due to hot corrosion and erosion. It is reported in the literature that 89 failures occurred in boilers in 1 year, out of which 50 failures

occurred due to hot corrosion and erosion [10]. Problems related to corrosion are not completely solved, but the cost related to corrosion can be decreased by 30% by using the different coating techniques.

Coatings are being used to increases the life of the materials, improve the performance, and also give a unique appearance [11–13]. Coatings reduce the corrosion rate to a great extent [14–16]. It is clear that 80% of the total investment to protect the metal from corrosion is related to coating applications [17, 18]. So, it is important to know all types of environment and many other conditions which degrade the material and preventive measure can be taken against them to ensure the reliability and safety in the use of metal components [19–21]. The use of protective coating has been increased to decrease the cost related to the maintenance of the component [22]. Applying coating on the material is the method to improve the life of the material and also balance their mechanical properties while protection against corrosion and erosion [23–25].

High-temperature erosion–corrosion is a serious problem in steam generation plants like gas turbines, IC engines, industrial waste incinerators, and boilers. It has been suggested by some researcher that by using different materials for boiler tubes together with Gr A1, T11, T22, T91, T92, Super 304H, and many different steels in numerous sections of the boilers in industries, the problem of hot corrosion was reduced

✉ Khushdeep Goyal
  khushgoyal@yahoo.com

1 Mechanical Engineering Department, Punjabi University, Patiala, India

2 Chitkara University Institute of Engineering and Technology, Chitkara University, Rajpura, India

to some extent. But, the research is constantly being done to enhance the performance of these materials with the aid of different coatings by the use of specific coating techniques or by way of introducing new materials for such applications. Literature review reveals that researchers have developed various types of coatings to improve corrosion resistance of boiler steel [26–34]. But the research of on NiCr–Cr_3C_2 coating is very limited. Therefore, it was decided to investigate performance of these distinct coatings on T22 boiler tube metal (low value material) in silicon tube furnace at 700 °C. The research was designed to study hot corrosion behaviour of boiler steel "ASTM-SA213-T22″ with different Cr_3C_2–NiCr coatings under molten salt environment in silicon tube furnace at 700 °C, under cyclic conditions, and to investigate the microstructure of corroded specimen by using XRD and SEM/EDAX techniques.

2 Materials and Methods

2.1 Substrate Materials

For this research work, T22 boiler steel material was selected to study hot corrosion behaviour. This material is currently being used in Guru Nanak Dev Thermal Plant Bathinda (Punjab), India. The spectroscopy of T22 boiler steel was done at Munjal castings Ludhiana (Punjab), India. The actual composition of T22 boiler steel is shown in Table 1.

Small pieces were cut from the rod of T22 boiler steel. The dimensions of steel specimen were approximately 20 mm × 15 mm × 5 mm. The specimens were polished by SiC emery paper 200, 600, 800, 1000.

2.2 Development of Coating

The material used for coating was Cr_3C_2–NiCr and this material was available in powder form. The Cr_3C_2–NiCr coatings were deposited at M/S Metallizing Equipment Co. Pvt. Ltd., Jodhpur (India). Different types of coatings were deposited on the specimens. The designation and chemical composition of these coatings is shown in Table 2.

Before the deposition of the coating, Al_2O_3 (Grit 60) was used for grit blasting the specimens. Coating deposited at M/S Metallizing Equipment Co. Pvt. Ltd., Jodhpur (India). Liquefied petroleum gas (LPG) was used as a fuel. During and after coating specimens were cooled with the help of compressed air jets.

Table 2 Different types of coatings

Coating designation	% of NiCr	% of Cr_3C_2
Coating 1	65	35
Coating 2	80	20
Coating 3	90	10
Coating 4	100	0

2.3 Exposure in Silicon Tube Furnace Environment

The coated as well as uncoated specimens were exposed to 700 °C in silicon tube furnace. About 700 °C was the average temperature with the variation of ± 5 °C. Each cycle consisted of 1 h heating followed by 20 min cooling at ambient conditions. At the end of each cycle, to analyse the surface texture visual observation of each specimen was done. After the visual observation, it has been washed out by acetone and the weight of specimen was taken using Electronic balance (CB-120, Contech Instruments Ltd., accuracy 0.001 g). After the 50 cycles, resulting specimens were analysed by visual examination, weight changes studies, SEM/EDAX, and XRD analysis.

3 Results

3.1 Visual Examination

The behaviour of uncoated "ASTM-SA213-T22" boiler after exposing to 700 °C for 50 cycles was visually examined. All the specimens were exposed in silicon tube furnace at elevated temperature. After 5th cycle, spalling of specimen was started, which increased with the increase in the number of cycles. At the end of the 20th cycle, peeling started and continued till the end of 50 cycles. At the end of 50th cycle, surface of the piece got distorted. The image of uncoated specimen after 50 cycles is shown in Fig. 1a. When coated specimen $35Cr_3C_2$–65NiCr was exposed to 700 °C for 50 cycles, at the end of 5th cycle, the shine on the surface was observed and white colour was observed after 15 cycles. The grey spots were seen on the surface after 20 cycles, and spalling of the specimen started at the end of 30th cycle. At the end of 50, the coating of specimen was found completely destroyed. The image of the $35Cr_3C_2$–65NiCr-coated specimen is shown in Fig. 1b. Another coated specimen

Table 1 Actual chemical composition (wt%) for T22 boiler tube steel used in the present study

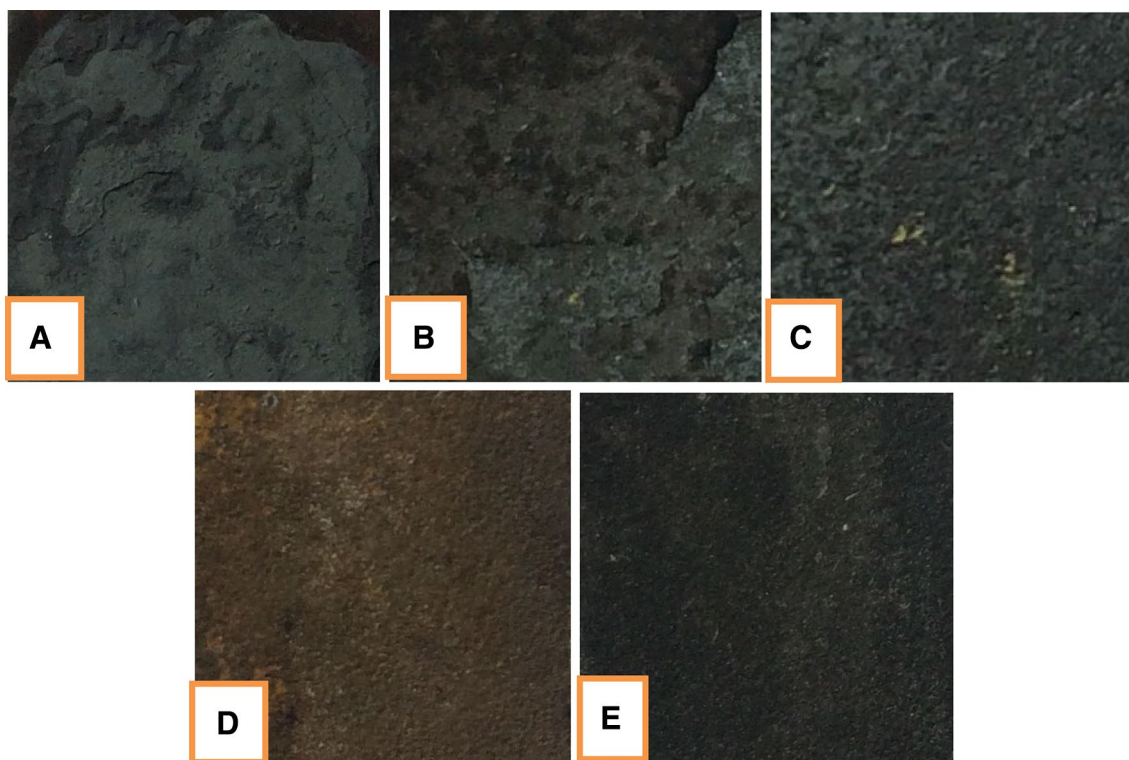| Type of steel	C	Mn	Si	P	S	Cr	Mo	Ni	Fe
T22	0.20	0.66	0.31	0.033	0.031	0.53	1.32	0.052	Balance

Fig. 1 Macrographs of specimens **a** Uncoated T22, **b** $35Cr_3C_2$–$65NiCr$, **c** $20Cr_3C_2$–$80NiCr$, **d** $10Cr_3C_2$–$90NiCr$, **e** $100NiCr$ after studied the hot corrosion behaviour in molten salt environment under cyclic conditions

$20Cr_3C_2$–$80NiCr$ was also exposed to 700 °C for 50 cycles. Coating started degrading after the 1st cycle and as the number of cycles increased, the spalling of the specimen increased. At the end of the 50 cycles, the coating from the corners of the specimen was found to be destroyed. The image of $20Cr_3C_2$–$80NiCr$-coated specimen is shown in Fig. 1c. Another coated specimen $10Cr_3C_2$–$90NiCr$ when exposed to 700 °C for 50 cycles turned yellowish in colour after 5th cycle and sides got spalled at the end of the 30th cycle. The image of $10Cr_3C_2$–$90NiCr$ is shown in Fig. 1d. Last coated specimen $100NiCr$ when exposed to 700 °C for 50 cycles showed better results as compared to other coatings. At the end of 30th cycle, reddish and brownish colour was noted on surface and after the 50th cycle it was observed that the coating of the specimen was safe. The image of 100%NiCr-coated specimen is shown in Fig. 1e.

3.2 Thermogravimetric Study

The thermogravimetric study was done for uncoated, $35Cr_3C_2$–$65NiCr$, $20Cr_3C_2$–$80NiCr$, $10Cr_3C_2$–$90NiCr$, and $100NiCr$ for low temperature (700 °C) hot corrosion. Weight changes per unit area (mg/cm^2) versus time expressed in number of cycles for uncoated and coated T22 boiler steel after exposing to the molten salt environment

($60V_2O_5$–$40Na_2SO_4$) in a silicon tube furnace at 700 °C for 50 cycles is presented in Fig. 2. From the graph, it is observed that the uncoated, $35Cr_3C_2$–$65NiCr$, and $100NiCr$ showed the high rate of corrosion as compared to $20Cr_3C_2$–$80NiCr$ and $10Cr_3C_2$–$90NiCr$, which means that $20Cr_3C_2$–$80NiCr$ and $10Cr_3C_2$–$90NiCr$-coated specimen provided the higher
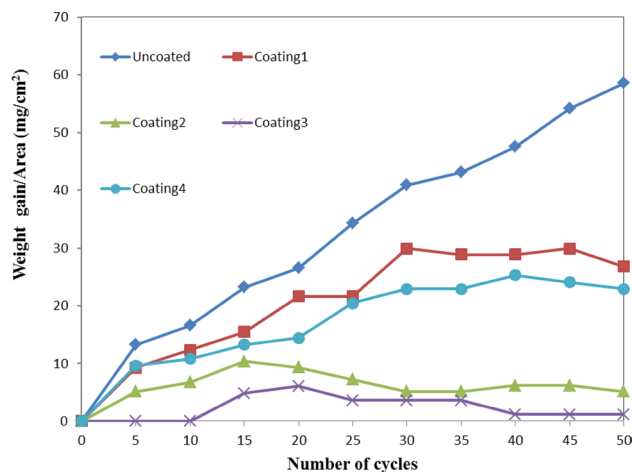

Fig. 2 Weight gain/area versus time (number of cycles) for the uncoated and coated specimen during the experimentation
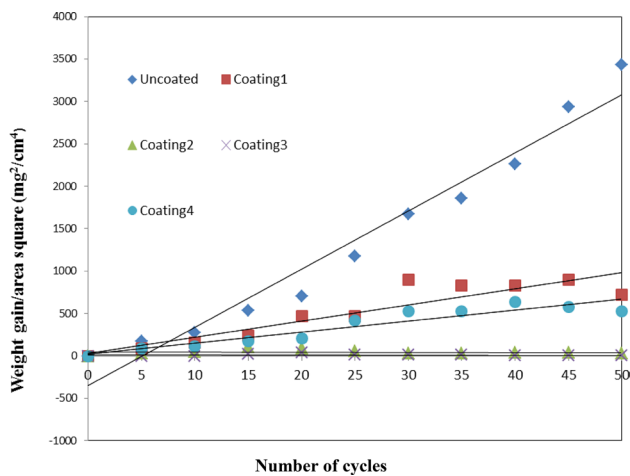
Fig. 3 (Weight gain/area)^2 versus time (number of cycles) for the uncoated and coated specimens during the experimentation where Coating $1 = 35Cr_3C_2$–$65NiCr$ coating, Coating $2 = 20Cr_3C_2$–$80NiCr$ coating, Coating $3 = 10Cr_3C_2$–$90NiCr$ coating, Coating $4 = 100NiCr$ coating

resistance to corrosion as compared to uncoated and other coated specimens. The cumulative weight change square per unit area (mg^2/cm^4) for 50 cycles is shown in Fig. 3. The cumulative weight change square after 50 cycles of hot corrosion for uncoated, $35Cr_3C_2$–$65NiCr$, and $100NiCr$ were found to be 3430, 714, and 469 mg^2/cm^4, respectively, while the weight change square for $20Cr_3C_2$–$80NiCr$ and $10Cr_3C_2$–$90NiCr$ were 4 and 1 mg^2/cm^4.

3.3 XRD Analysis of T22 Uncoated and Coated After Exposed at 700 °C in Molten Salt Environment

T22-uncoated and HVOF-coated specimens after exposed to 700 °C in molten salt environment in silicon tube furnace were analysed by X-ray diffraction technique. The XRD analysis of uncoated specimen shows the presence of Fe_2O_3 after exposure to molten salt environment for 50 cycles. The XRD analysis of HVOF-coated specimens shows the presence of (a) Ni, (b) Cr, (c) NiC, (d) Cr_3C_2. The presence of Cr_3C_2 on the surface of the coated specimens helps to resist the corrosion. The XRD analysis of T22 uncoated and coated specimens is shown in Fig. 4.

3.4 SEM/EDAX Analysis of T22 Uncoated and Coated After Exposed at 700 °C in Molten Salt Environment

SEM/EDAX analysis of T22-uncoated and coated specimens were done after exposed to 700 °C in molten salt environment. SEM/EDAX analysis of T22-uncoated specimen shows the formation of Fe and O on the surface of the specimen as the main elements and these elements form Fe_2O_3.
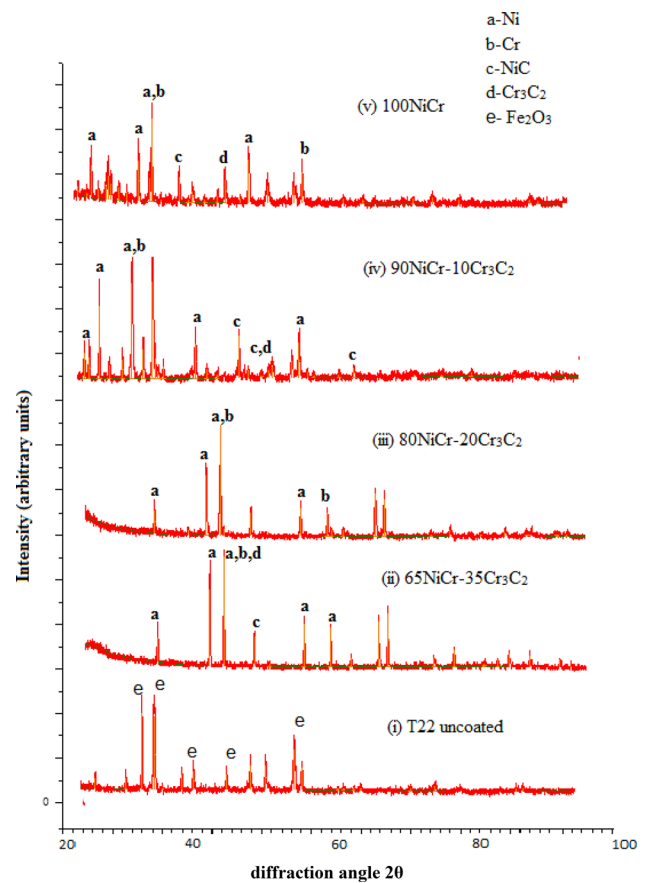

Fig. 4 XRD analysis of T22-uncoated and HVOF-coated specimens

SEM/EDAX analysis of coated specimens shows the occurrence of Cr, O, and C as main element. SEM/EDAX analysis of uncoated and coated specimens is shown in Fig. 5.

4 Discussion

The high rate of corrosion was indicated by the macrographs of T22 uncoated, $35Cr_3C_2$–$65NiCr$, and $100NiCr$. The weight changes graphs showed the high change in weight for T22 uncoated, $35Cr_3C_2$–$65NiCr$, and $100NiCr$ during exposure to molten salt environment in silicon tube furnace at 700 °C. The reason for high change in weight was the formation of Fe_2O_3 on the surface of T22-uncoated specimen. The macrographs of uncoated specimen show that the oxide scales which formed on the surface were porous in nature and this porous nature was responsible for the high rate corrosion of T22-uncoated specimen. XRD analysis also confirmed the formation of Fe_2O_3 for the T22-uncoated specimen after exposing to molten salt environment in silicon tube furnace at 700 °C and shows Fe_2O_3 as the main phase. SEM/EDAX analysis of T22-uncoated specimen shows the formation of Fe and O on the surface of the specimen as the
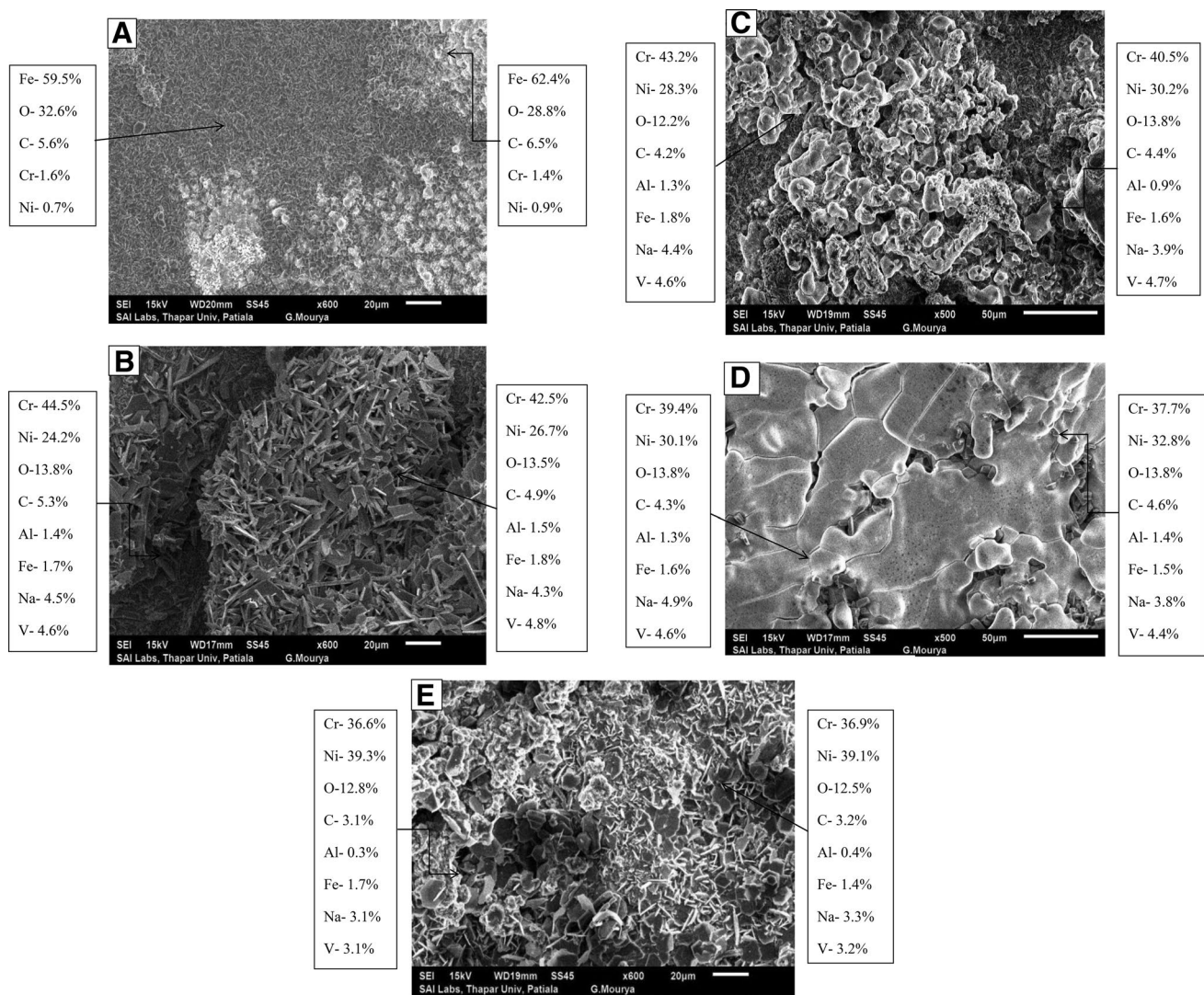
Fig. 5 SEM and EDAX analysis of **a** T22 uncoated, **b** 35Cr$_3$C$_2$–65NiCr, **c** 20Cr$_3$C$_2$–80NiCr, **d** 10Cr$_3$C$_2$–90NiCr, **e** 100NiCr after exposed to 700 °C in molten salt environment

main elements. The formation of oxides of iron has also been reported by various authors [32, 35–37]. The EDAX analysis also shows Ni and Cr in the scale, and these elements might have diffused from the base alloy at high temperature of exposure.

The coatings of 20Cr$_3$C$_2$–80NiCr-coated and 10Cr$_3$C$_2$–90NiCr-coated specimens were intact after exposure to molten salt environment in silicon tube furnace at 700 °C for 50 cycles. 20Cr$_3$C$_2$–80NiCr-coated and 10Cr$_3$C$_2$–90NiCr-coated specimens provided the high resistance to corrosion and did not show oxidation attack. The smooth scale was formed on the surfaces of these two coated specimens. The penetration of corrosive species was resisted by splats parallel to the substrate surface [5, 38]. The weight changes graph shows that the 20Cr$_3$C$_2$–80NiCr-coated and 10Cr$_3$C$_2$–90NiCr-coated specimens were capable of reducing the weight change as compared to uncoated, 35Cr$_3$C$_2$–65NiCr-coated, and 100NiCr-coated specimen. The lowest weight change was found for 10Cr$_3$C$_2$–90NiCr-coated specimen, whereas the highest weight change was found for 35Cr$_3$C$_2$–65NiCr among different types of coatings used. The XRD analysis of coated specimens shows the occurrence of (a) Ni, (b) Cr, (c) NiCr, and (d) Cr$_3$C$_2$ after exposing to molten salt environment in silicon tube furnace at 700 °C.

The coated specimens 100NiCr, 10Cr$_3$C$_2$–90NiCr, and 35Cr$_3$C$_2$–65NiCr show the presence of (a) Ni and (b) Cr. The formation of NiC and Cr$_3$C$_2$ might be the reason for lower corrosion rate of these coatings as compared to T22-uncoated specimen. The development of Cr$_3$C$_2$ on the surface of 100NiCr-coated, 10Cr$_3$C$_2$–90NiCr-coated, and 35Cr$_3$C$_2$–65NiCr-coated specimens was further analysed by

SEM/EDAX and showed Cr, O, and C as the main elements after exposing to molten salt environment in silicon tube furnace at 700 °C. The rate of weight gain of coated specimens was reduced in comparison to uncoated specimen by providing the high resistance to corrosive species. SEM/EDAX analysis traced the presence of Ni and Cr on the surface of coated specimens; this was due to penetration of these elements to the coating surface from substrate at low temperature (700 °C) in molten salt environment.

5 Conclusions

The following conclusions are drawn from this experimental study:

- $35Cr_3C$–$65NiCr$, $20Cr_3C$–$80NiCr$, $10Cr_3C$–$90NiCr$, and $100NiCr$ coatings were deposited by HVOF-sprayed technique.
- During the coating of T22 boiler steel specimens, oxygen was diffused into coating.
- All the coatings used in study provide the better resistance to corrosion in molten salt environment when exposed for 50 cycles in silicon tube furnace. The sequence of coatings provided the resistance to corrosion in decreasing order shown below:

    $10Cr_3C_2$-$90NiCr$-coated T22 > $20Cr_3C_2$–$80NiCr$-coated T22 > $100NiCr$-coated T22 > $35Cr_3C_2$–$65NiCr$-coated T22.
- Uncoated T22 specimen shows the highest change in weight during the exposure to hot corrosion.
- Spalling and peeling of uncoated T22 during the exposure to molten salt environment in silicon tube furnace at 700 °C. Formation of Fe_2O_3 on the surface of uncoated T22.
- $10Cr_3C_2$–$90NiCr$ and $20Cr_3C_2$–$80NiCr$ coatings provided the higher resistance to corrosion as compared to $100NiCr$ and $35Cr_3C_2$–$65NiCr$. The formation of chromium carbide layer on the coated surface protects them from corrosion.

Compliance with Ethical Standards

References

1. Singh G, Goyal K, Bhatia R (2018) Hot corrosion studies of plasma-sprayed chromium oxide coatings on boiler tube steel at 850 °C in simulated boiler environment. Iran J Sci Technol Trans Mech Eng 42(2):149

2. Saladi S, Menghani JV, Prakash S (2015) Characterization and evaluation of cyclic hot corrosion resistance of detonation-gun sprayed Ni-5 Al coatings on inconel-718. J Therm Spray Technol 24(5):778

3. Dobrzański L, Lukaszkowicz K, Zarychta A, Cunha L (2005) Corrosion resistance of multilayer coatings deposited by PVD techniques onto the brass substrate. J Mater Process Technol 164:816

4. Goyal K, Singh H, Bhatia R (2016) Current status of thermal spray coatings for high temperature corrosion resistance of boiler steel. J Mater Metall Eng 6(1):29

5. Zhou W, Zhou K, Li Y, Deng C, Zeng K (2017) High temperature wear performance of HVOF-sprayed Cr_3C_2-WC-NiCoCrMo and Cr_3C_2-NiCr hardmetal coatings. Appl Surf Sci 416:33

6. Goyal K, Singh H, Bhatia R (2018) Effect of carbon nanotubes on properties of ceramics based composite coatings. Adv Eng Forum 26:53

7. Chatha SS, Sidhu HS, Sidhu BS (2016) Performance of $75Cr_3C_2$-$25NiCr$ coating produced by HVOF process in a coal-fired thermal power plant. Adv Mater Res 1137:88

8. Goyal K, Singh H, Bhatia R (2018) Mechanical and microstructural properties of carbon nanotubes reinforced chromium oxide coated boiler steel. World J Eng 15(4):429

9. Kaur M, Singh H, Prakash S (2009) High-temperature corrosion studies of HVOF-sprayed Cr_3C_2-NiCr coating on SAE-347H boiler steel. J Therm Spray Technol 18(4):619

10. Chatha SS, Sidhu HS, Sidhu BS (2012) High temperature hot corrosion behaviour of NiCr and Cr_3C_2–NiCr coatings on T91 boiler steel in an aggressive environment at 750 °C. Surf Coat Technol 206(19–20):3839

11. Kaewsai D, Watcharapasorn A, Singjai P, Wirojanupatump S, Niranatlumpong P, Jiansirisomboon S (2010) Thermal sprayed stainless steel/carbon nanotube composite coatings. Surf Coat Technol 205(7):2104

12. Goyal K, Singh H, Bhatia R (2019) Behaviour of carbon nanotubes-Cr_2O_3 thermal barrier coatings in actual boiler. Surf Eng. https://doi.org/10.1080/02670844.2019.1584966

13. Hemmati A, Soltanieh S, Masoudpanah S (2018) On the Interaction between erosion and corrosion in chromium carbide coating. J Bio Tribo-Corros 4(1):10

14. Rezakhani D (2007) Corrosion behaviours of several thermal spray coatings used on boiler tubes at elevated temperatures. Anticorros Methods Mater 54(4):237

15. Maiti A, Mukhopadhyay N, Raman R (2007) Effect of adding WC powder to the feedstock of WC–Co–Cr based HVOF coating and its impact on erosion and abrasion resistance. Surf Coat Technol 201(18):7781

16. Singh H, Puri D, Prakash S (2005) Some studies on hot corrosion performance of plasma sprayed coatings on a Fe-based superalloy. Surf Coat Technol 192(1):27

17. Chawla V, Puri D, Prakasha S, Chawla A, Sidhu BS (2009) Characterization and comparison of corrosion behavior of nanostructured TiAlN and AlCrN coatings on superfer 800H (INCOLOY 800 H) substrate. J Miner Mater Charact Eng 8(09):715

18. Sidhu VPS, Goyal K, Goyal R (2017) Comparative study of corrosion behaviour of HVOF-coated boiler steel in actual boiler environment of a thermal power plant. J Aust Ceram Soc 53(2):925

19. Clarke DR, Oechsner M, Padture NP (2012) Thermal-barrier coatings for more efficient gas-turbine engines. MRS Bull 37(10):891

20. da Silva F, Bedoya J, Dosta S, Cinca N, Cano I, Guilemany J et al (2017) Corrosion characteristics of cold gas spray coatings of reinforced aluminum deposited onto carbon steel. Corros Sci 114:57

21. Doolabi MS, Ghasemi B, Sadrnezhaad S, Habibollahzadeh A, Jafarzadeh K (2017) Hot corrosion behavior and near-surface microstructure of a "low-temperature high-activity Cr-aluminide"

coating on inconel 738LC exposed to Na_2SO_4, $Na_2SO_4 + V_2O_5$ and $Na_2SO_4 + V_2O_5 + NaCl$ at 900° C. Corros Sci 128:42

22. Goyal K, Singh H, Bhatia R (2018) Experimental investigations of carbon nanotubes reinforcement on properties of ceramic-based composite coating. J Aust Ceram Soc 55:315

23. Huang S, Sun D, Wang W (2015) Microstructures and properties of Ni based composite coatings prepared by plasma spray welding with mixed powders. Int J Refract Metal Hard Mater 52:36

24. Irissou E, Legoux J-G, Arsenault B, Moreau C (2007) Investigation of Al-Al_2O_3 cold spray coating formation and properties. J Therm Spray Technol 16(5–6):661

25. Karthikeyan J, Sreekumar K, Venkatramani N, Rohatgi V (1988) Preparation and characterization of plasma-sprayed thick ceramic coatings reinforced with metal pins. High Temp High Press 20(6):653

26. Tianshun D, Xiukai Z, Guolu L, Li L, Ran W (2018) Microstructure and corrosive wear resistance of plasma sprayed Ni-based coatings after TIG remelting. Mater Res Express 5(2):026411

27. Mistry JM, Gohil PP (2018) Research review of diversified reinforcement on aluminum metal matrix composites: fabrication processes and mechanical characterization. Sci Eng Compos Mater 25(4):633

28. Fauchais P, Vardelle M, Vardelle A, Goutier S (2018) Sprays used for thermal barrier coatings. Applications paradigms of droplet and spray transport: paradigms and applications. Springer, Singapore, p 311

29. Xu S, Chen L, Gong M, Hu X, Zhang X, Zhou Z (2017) Characterization and engineering application of a novel ceramic composite insulation material. Composites B 111:143

30. Ozgurluk Y, Doleker KM, Karaoglanli AC (2017) Hot corrosion behavior of YSZ, $Gd_2Zr_2O_7$ and YSZ/$Gd_2Zr_2O_7$ thermal barrier coatings exposed to molten sulfate and vanadate salt. Appl Surf Sci 438:96–113

31. Keyvani A, Bahamirian M (2017) Hot corrosion and mechanical properties of nanostructured Al_2O_3/CSZ composite TBCs. Surf Eng 33(6):433

32. Sidhu VPS, Goyal K, Goyal R (2017) An investigation of corrosion resistance of HVOF coated ASME SA213 T91 boiler steel in an actual boiler environment. Anticorros Methods Mater 64(5):499

33. Goyal K, Singh H, Bhatia R (2018) Cyclic high temperature corrosion studies of carbon nanotubes-Cr_2O_3 composite coatings on boiler steel at 900 °C in molten salt environment. Anticorros Methods Mater 65(6):646

34. Goyal K, Singh H, Bhatia R (2019) Hot-corrosion behavior of Cr_2O_3-CNT-coated ASTM-SA213-T22 steel in a molten salt environment at 700°C. Int J Miner Metall Mater 26(3):337

35. Goyal K, Singh H, Bhatia R (2018) Hot corrosion behaviour of carbon nanotubes reinforced chromium oxide composite coatings at elevated temperature. Mater Res Express 5(11):116408

36. Manikandan DWM (2018) High-temperature corrosion behaviour of HVOF sprayed Cr3C2-25NiCr coated on alloy X22CrMoV12-1 at 600 °C. J Therm Spray Eng 1(1):7

37. Khan MA, Sundarrajan S, Natarajan S (2017) Hot corrosion behaviour of super 304H for marine applications at elevated temperatures. Anticorros Methods Mater 64(5):508

38. Kaplan M, Uyaner M, Ozgurluk Y, Doleker KM, Karaoglanli AC (2019) Evaluation of hot corrosion behavior of APS and HVOF sprayed thermal barrier coatings (TBCs) exposed to molten $Na_2SO_4 + V_2O_5$ salt at 1000 °C. Engineering design applications. Springer, Cham, p 441